Experimental Animals
Exp. Anim. 72(3), 413–424, 2023

Original

Loss of N-acetylglucosaminyl transferase V is involved in the impaired osteogenic differentiation of bone marrow mesenchymal stem cells

Xiao-Po LIU[1, 2], Jia-Qi LI[1], Ruo-Yu LI[1], Guo-Long CAO[2], Yun-Bo FENG[2] and Wei ZHANG[1]

[1]*Department of Spinal Surgery, The Third Hospital of Hebei Medical University, No. 139, Ziqiang Road, Shijiazhuang 050051, Hebei, P.R. China*
[2]*Department of Orthopedics, Tangshan Gongren Hospital, No. 27, Wenhua Road, Tangshan 063000, Hebei, P.R. China*

Abstract: The imbalance of bone resorption and bone formation causes osteoporosis (OP), a common skeletal disorder. Decreased osteogenic activity was found in the bone marrow cultures from N-acetylglucosaminyl transferase V (MGAT5)-deficient mice. We hypothesized that MGAT5 was associated with osteogenic differentiation of bone marrow mesenchymal stem cells (BMSCs) and involved in the pathological mechanisms of osteoporosis. To test this hypothesis, the mRNA and protein expression levels of MGAT5 were determined in bone tissues of ovariectomized (OVX) mice, a well-established OP model, and the role of MGAT5 in osteogenic activity was investigated in murine BMSCs. As expected, being accompanied by the loss of bone mass density and osteogenic markers (runt-related transcription factor 2, osteocalcin and osterix), a reduced expression of MGAT5 in vertebrae and femur tissues were found in OP mice. *In vitro*, knockdown of *Mgat5* inhibited the osteogenic differentiation potential of BMSCs, as evidenced by the decreased expressions of osteogenic markers and less alkaline phosphatase and alizarin red S staining. Mechanically, knockdown of *Mgat5* suppressed the nuclear translocation of *β*-catenin, thereby downregulating the expressions of downstream genes *c-myc* and axis inhibition protein 2, which were also associated with osteogenic differentiation. In addition, *Mgat5* knockdown inhibited bone morphogenetic protein (BMP)/transforming growth factor (TGF)-β signaling pathway. In conclusion, MGAT5 may modulate the osteogenic differentiation of BMSCs via the *β*-catenin, BMP type 2 (BMP2) and TGF-β signals and involved in the process of OP.

Key words: bone marrow mesenchymal stem cells (BMSCs), bone morphogenetic protein (BMP)/transforming growth factor (TGF)-β, N-acetylglucosaminyl transferase V (MGAT5), osteoporosis, ovariectomized mice, Wnt/*β*-catenin

Introduction

Osteoporosis (OP) is one of the common systemic skeletal diseases which is characterized by low bone mass, leading to a microarchitectural deterioration of bone tissue [1, 2]. Over 75 million people worldwide suffer from this disease, of which 80% are postmenopausal women and this number is gradually increasing [3]. Recently, lack of estrogen has been admitted as the main pathogenic mechanism of postmenopausal OP development [4, 5]. Estrogen deficiency damages normal bone remodeling via increasing resorption activity of osteoclasts. The bone resorption is greater than the bone formation, thereby causing loss of bone [6]. At present, the medicinal treatments for OP included calcitonin, bisphosphonates (alendronate) and estrogen replacement [7–9]. However, these drugs have side effects and limitations after long-term treatment, including atypical femur fracture and jaw necrosis [10, 11]. Individuals with OP were at a higher risk of bone fragility and frac-

(Received 20 September 2022 / Accepted 30 March 2023 / Published online in J-STAGE 5 April 2023)
Corresponding author: W. Zhang. email: zhangweiat408@sina.com

ture [12]. Fractures caused by OP lead to pain and dysfunction along with an enormous socioeconomic burden [3]. So it was necessary to explore the novel treatment factors for postmenopausal OP.

The imbalance between fat mass and bone was a representative feature of the pathogenesis of OP [13]. Bone marrow mesenchymal stem cells (BMSCs) are stem cells that have multiple differentiation abilities and self-renewal capacity [14]. As the main origins of adipocytes and osteoblasts, BMSCs maintain a balance between them [15, 16]. The abnormal decrease of estrogen level disrupted the adipocyte and osteoblast differentiation balance and led to faulty bone metabolism, ultimately resulting in OP [17]. Therefore, the differentiation of BMSCs played an important role in OP and should be concerned.

N-acetylglucosaminyl transferase V (MGAT5), an important glycosyl transferase distributed in the Golgi apparatus, catalyzes the formation of β-1, 6 branches of N-glycans. It changes the sugar chain structure of cell surface glycoproteins such as cadherin. It affects autoimmune disease and cancer malignancy [18]. Cheung *et al.* demonstrated that *Mgat5*-deficient mice accelerated age-related loss of bone mineral density (BMD) in vertebrae and femur and in whole-body measurements [19]. However, its protective influence and mechanisms in postmenopausal OP remained unclear.

Herein, we focused on the function of MGAT5 in osteogenic differentiation of BMSCs, and tried to reveal its role in the developmental process of OP in OVX-induced mice.

Materials and Methods

Materials and reagents

Goat anti-rabbit IgG/HRP (1:3,000) and goat anti-mouse IgG/HPR (1:3,000) were provided by Solarbio (Beijing, China). MGAT5 antibody (1:1,000), runt-related transcription factor 2 (RUNX2) antibody (1:1,000), osteocalcin (OCN) antibody (1:1,000), osterix (OSX) antibody (1:2,000), β-catenin antibody (1:3,000), transforming growth factor-β1 (TGF-β1) antibody (1:1,000), p-SMAD2/3 antibody (1:1,000), and SMAD2/3 antibody (1:1,000) were provided by ABclonal (Shanghai, China). Bone morphogenetic protein type 2 (BMP2) antibody (1:1,000), p-SMAD1 antibody (1:1,000) and SMAD1 antibody (1:1,000) were purchased from Affinity Biosciences LTD. (Melbourne, Australia). Histone H3 antibody (1:10,000) and GAPDH antibody (1:20,000) were obtained from Proteintech Group, Inc. (Rosemont, IL, USA).

Ovariectomized (OVX) operation in mice

All animal experiments were followed the Guideline for the Care and Use of Laboratory Animals. And they were ratified by the Ethics Committee of Tangshan Gongren Hospital (GRYY-LL-2020-84). Seven-week-old female C57BL/6J mice were provided *ad libitum* access to water and a standard rodent diet. The mice were housed in pathogen-free conditions at a temperature of 22 ± 1°C and humidity of 45–55% under a 12/12 h light/dark cycle. After a week of acclimation, the mice were randomly divided into the control and OP group. After being anesthetized, mice in the OP group received a bilateral ovariectomy and the mice in the sham group received a sham procedure with the ovaries left. Then the abdominal musculature and skin were closed. Six weeks post-operatively, the mice were deep anesthetized with sevoflurane for blood and bone tissue collection.

Micro-computed tomography (CT) analysis

Femur samples were scanned with Quantum GX micro-CT system (PerkinElmer, Massachusetts, USA) at a voxel size of 10 μm. Quantum and Caliper Analyze software provided with the instrument were used for scan and analysis. BMD, ratio of bone volume to total volume (BV/TV) and trabecular number (Tb.N) were calculated.

Bone histomorphometry

Femur was collected and fixed with 4% paraformaldehyde. After dehydration, embedment and being cut to slices (5 μm), the slices were stained with toluidine blue. Analyses of the osteoclast number (N.Oc), osteoclast surface (Oc.S), osteoblast number (N.Ob), and osteoblast surface (Ob.S) were performed using staining results.

Isolation, culture and identification of BMSCs

Primary BMSCs were harvested from femur and tibia of 8-week-old mice. The bones were crushed and digested in phosphate buffer (PBS) supplemented with 1 mg/ml type IV collagenase, 2 mg/ml neutral protease II, and 1% bovine serum albumin (BSA). The erythrocytes were lysed by red blood cell lysis buffer at room temperature. The supernatant was discarded, and the remaining cells were resuspended in modified eagle medium (MEM) α medium (iCell Bioscience Inc., Shanghai, China) containing 10% fetal bovine serum (FBS). The cells were cultured in a 37°C incubator with a 5% CO_2. After 24 h, non adherent cells were washed with PBS. The cells at passage 3 were used for the experiments. BMSCs were identified by flow cytometry to detect the typical markers including CD29, CD34, CD45 and CD90 (Biolegend, San Diego, CA, USA).

Lentiviral infection of BMSCs

To obtain recombinant plasmids, the shRNA sequences targeting *Mgat5* were inserted into the lentiviral vector (Hunan Fenghui Biotechnology Co., Ltd., Changsha, China). Lentiviral and assistant plasmids (Hunan Fenghui Biotechnology Co., Ltd., Changsha, China) were co-transfected into 293T cells to obtain the lentiviral particles. For infection, BMSCs were incubated with lentiviral particles in growth medium at a multiplicity of infection (MOI) of 50 at 37°C with 5% CO_2. And the BMSCs were collected after 48 h of infection for use in subsequent experiments.

Osteogenic, adipogenic and chondrogenic differentiation of BMSCs

BMSCs were planted onto culture plates. The cells were cultured in osteogenic, adipogenic or chondrogenic medium. The osteogenic medium was basic medium supplemented with 10% FBS, 10 mM β-sodium glycerophosphate, 50 μM L-lascorbic acid 2-phosphate, 100 ng/ml BMP2 and 1×10^{-4} mM dexamethasone (DEX). Alizarin red S (Shanghai yuanye Bio-Technology Co., Ltd., Shanghai, China) staining was performed after BMSCs were incubated with osteogenic medium for 14 d.

The adipogenic medium was consisted of dulbecco's modified eagle medium (DMEM) supplemented with 10% FBS, 1×10^{-4} mM DEX, 10 mM β-sodium glycerophosphate, 50 μM L-lascorbic acid 2-phosphate and 10 μg/ml insulin. Oil red O staining was performed after BMSCs were incubated with adipogenic medium for 14 d. Cells were fixed in cell ORO fixative for 15 min, washed with PBS, and stained with Oil red O staining solution (Leagene, Beijing, China) for 10 min.

The chondrogenic medium was composed of basic medium supplemented with 10% FBS, 50 μg/ml L-lascorbic acid 2-phosphate, 100 μg/ml sodium pyruvate, 40 μg/ml proline, 10 ng/ml TGF-β1, 1×10^{-4} mM DEX and 100 ng/ ml insulin-like growth factor (IGF)-1. The cells were seeded into cell climbing. The cell climbing was washed with distilled water incubated with Alcian acidizing fluid for 3 min and incubated with Alcian blue (Leagene, Beijing, China) for 15 min. Then cell climbing was washed with distilled water for 5 min. Nuclear fast red staining solution was used to stain nuclei for 10 min. After rinsing, the cell climbing was added glycerol-alcohol and sealed at low temperature. The cells were observed under a light microscope.

Alkaline phosphatase (ALP) activity and ALP staining assay

ALP activity of serum and cell supernatant was analyzed using the ALP assay kit purchased from Nanjing Jiancheng Bioengineering Institute (Nanjing, China) according to the manufacturer's instructions. After 7 days of osteoblastic induction, cells were stained by an ALP staining kit (Solarbio) and observed under a light microscope.

Quantitative Real-time PCR (qPCR)

Total RNA was extracted from the tissues and BMSCs using a Trizol reagent (BioTeke Corp., Beijing, China). The absorbance of total RNA was measured to determine the purity and concentration. The cDNA was synthesized using BeyoRT^{TM} II M-MLV reverse transcriptase (Beyotime, Shanghai, China). qPCR was performed using SYBR Green qPCR Master Mix (Solarbio) under the following cycling conditions: 95°C for 5 min followed by 40 cycles of 95°C for 10 s, 60°C for 10 s and 72°C for 15 s. Gene expression levels were determined by the $2^{-\Delta\Delta Ct}$ method and *Gapdh* was used as the internal control gene. The PCR primers were provided in Table 1.

Western blotting analysis

Total protein of vertebrae, femur or BMSCs was extracted using the radio immunoprecipitation assay (RAPI) lysis buffer (Solarbio) and was quantified using a bicinchoninic acid (BCA) protein assay kit (Solarbio). Equal amounts of proteins were separated by SDS-PAGE and transferred to a polyvinylidene fluoride (PVDF) membrane (Millipore, Billerica, MA, USA). Membranes were blocked with 5% non-fat milk (Sangon, Shanghai, China) for 1 h and were incubated with the primary antibodies at 4°C overnight. After washing in Tris-buffered

Table 1. Primer names and sequences for qPCR analysis

Primer Name	Forward	Reverse
Mgat5	5'-CAGCTCCATGTTACGGG-3'	5'-GACCAGATTGTCCACCTTT-3'
Axin2	5'-CAACGACAGCGAGTTATCC-3'	5'-GTTCCACAGGCGTCATCT-3'
c-myc	5'-GGACTGTATGTGGAGCGGTTTC-3'	5'-TCGTTGAGCGGGTAGGGA-3'
Ocn	5'-GAGGGCAATAAGGTAGTGAA-3'	5'-CATAGATGCGTTTGTAGGC-3'
Runx2	5'-GCAGCACTCCATATCTCTACT-3'	5'-TTCCGTCAGCGTCAACAC-3'
Osx	5'-ACCAGGTCCAGGCAACA-3'	5'-AGCAAAGTCAGATGGGTAAGT-3'
Alp	5'-GACAGCAAGCCCAAGAG-3'	5'-GGAGACGCCCATACCA-3'
Gapdh	5'-TGTTCCTACCCCCAATGTGTCCGTC-3'	5'-CTGGTCCTCAGTGTAGCCCAAGATG-3'

saline with Tween (TBST) for 10 min, the membranes were incubated with secondary antibody at 37°C for 1 h. Protein bands were visualized by ECL reagent (Solarbio) and images were analyzed by Gel-Pro-Analyzer software.

Statistical analysis

One-way ANOVA and *t* tests were performed to analyze the data with GraphPad Prism 8 software. Data were presented as mean ± SD. A *P*-values of <0.05 was considered statistically significant.

Results

Downregulation of MGAT5 expression in OP mice

The microstructures of femurs in each group were analyzed by micro-CT. As demonstrated in Fig. 1a, the BMD, BV/TV and Tb.N were significantly lower in the OP group 6 weeks after the surgery compared to the control group ($P<0.001$). N.Oc and Oc.S were increased, and N.Ob and Ob.S were reduced in the OVX model (Table 2). Our data revealed that the bone resorption was increased and the bone formation was reduced in the mice with OP. Meanwhile, reduced *Alp* mRNA was observed in the OP group (Fig. 1b). Interestingly, the ALP activity was increased in OP mice (Fig. 1b). Additionally, mRNA and protein expression levels of MGAT5 in the vertebrae and femur were both remarkably reduced in the mice with OP (Figs. 1c and d). As shown in Figs. 1e and f, the mRNA and protein expression of RUNX2, OCN and OSX were decreased in the OP mice. These data revealed that MGAT5 might be involved in the development of OP.

Up-regulated expression of MGAT5 during the osteogenic differentiation and mineralization of BMSCs

The BMSCs were successfully isolated from mice with high purity, which was proved by the high expressions of MSCs surface markers CD29 (89.34%) and CD90 (96.39%), low expression of the hematopoietic markers CD34 (1.14%) and CD45 (0.85%) (Fig. 2a), and osteogenic, adipogenic and chondrogenic differentiation abilities (Fig. 2b).

We investigated the expression changes of MGAT5 during the osteogenic differentiation of BMSCs. As shown in Figs. 3a and b, when incubated in osteogenic differentiation medium, the BMSCs showed dramatical increases in mRNA and protein expression of MGAT5 at day 7. Notably, these increases were accompanied by the upregulated expressions of osteogenic markers *Runx2*, *Ocn*, and *Osx* (Fig. 3c) and greater ALP staining (Fig. 3d), which meant the initiation of osteogenic differentiation. In addition, the increases of MGAT5 were maintained to day 14, the time point that mineralization occurred. The differentiation formed many mineralized nodules with small size in the visual field at this time point (Fig. 3e).

Mgat5 knockdown inhibited osteogenic differentiation of BMSCs

To clarify the function of MGAT5 in BMSCs osteogenic differentiation, *Mgat5* was knocked down by lentivirus. Results of qPCR and western blot demonstrated that expressions of MGAT5 were efficiently knocked down in both undifferentiated and differentiated BMSCs (Figs. 4a–c).

When *Mgat5* was knocked down, the mRNA and protein expression levels of RUNX2, OCN and OSX were noticeably downregulated compared to the lenti-control treated BMSCs (Figs. 4d and e). Meanwhile, ALP staining was markedly reduced and ALP activity was significantly suppressed in the knockdown of *Mgat5* treated cells (Figs. 4f and g), suggesting the impaired osteogenic differentiation ability of BMSCs. At day 14, fewer calcium nodule formation was observed in the *Mgat5* silenced cells (Fig. 4h). As shown in Fig. 4i, lipid droplet formation in *Mgat5* silenced cells was enhanced, when compared with lenti-control treated cells. These results showed that loss of MGAT5 may suppress osteogenic differentiation and mineralization, and aggravate adipogenic differentiation.

Mgat5 knockdown inhibited the Wnt/*β*-catenin and BMP/TGF-*β* signaling pathways

To explore the pathological mechanism of MGAT5 loss-impaired osteogenic differentiation, we measured the activity of *β*-catenin and expressions of its downstream genes, a typical signaling pathway regulating osteogenic differentiation [20]. The protein level of *β*-catenin in the nucleus was significantly diminished in *Mgat5* silencing BMSCs (Fig. 5a), which indicated the nuclear translocation of *β*-catenin was reduced. Also, the mRNA expression levels of its downstream genes *c-myc* and axis inhibition protein 2 (*Axin2*) (Fig. 5b), which indicated the activity of this signaling pathway, was inhibited. These data revealed that *Mgat5* knockdown inhibited the Wnt/β-catenin signaling pathway. As shown in Figs. 5c and d, *Mgat5* knockdown decreased the expression of BMP2 and TGF-β1. The phosphorylation of SMAD1 and SMAD2/3 was also reduced in *Mgat5* silencing BMSCs. These findings suggested that BMP/TGF-β signaling may be involved in the MGAT5-associated osteogenic differentiation of BMSCs.

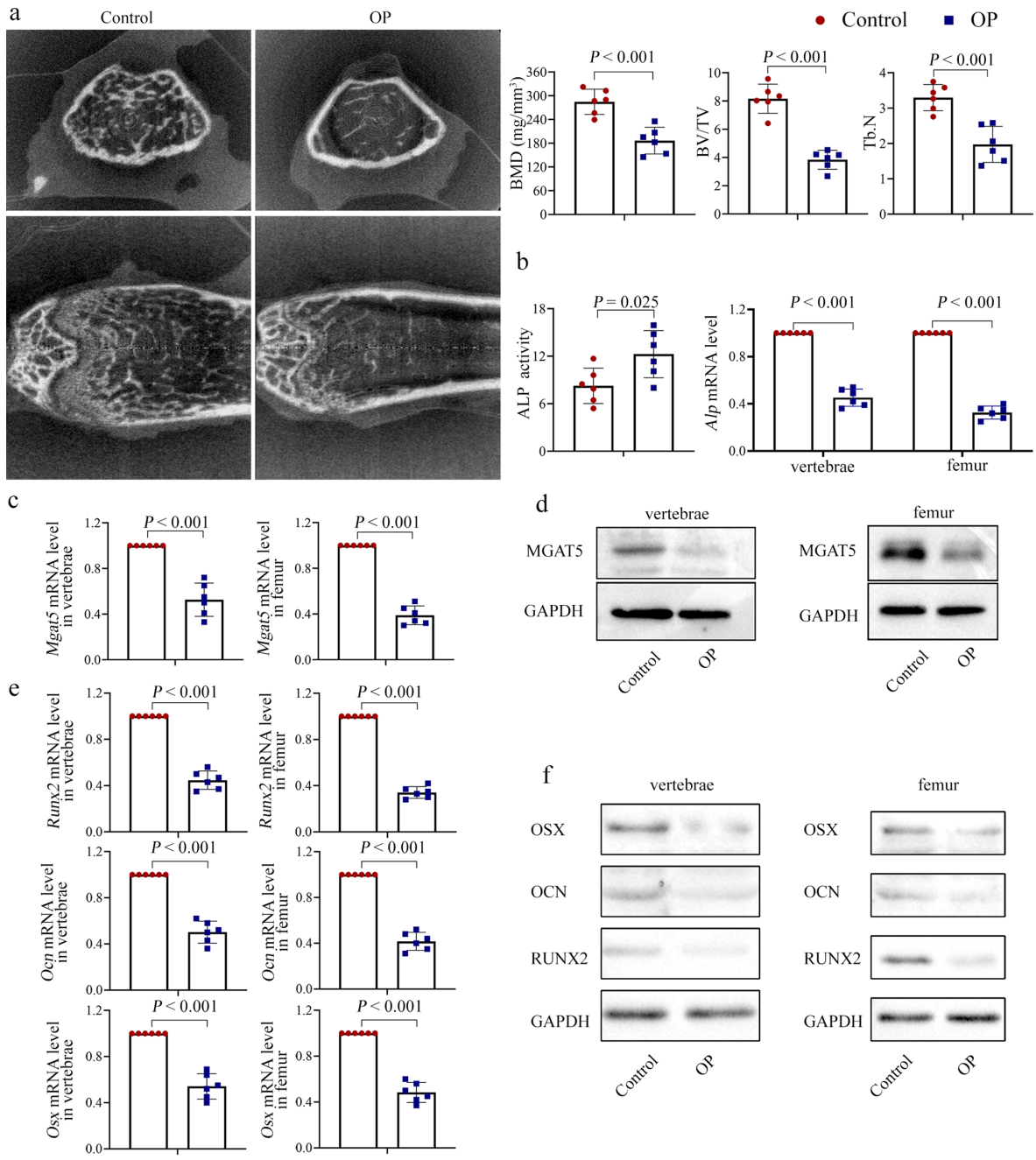

Fig. 1. Downregulation of MGAT5 expression in OP mice. (a) Representative micro-CT images of femur bone and quantitative analyses of bone structural parameters, including BMD, BV/TV, and Tb.N. (b) qPCR was used to detect the mRNA level of *Alp* in vertebrae and femur. ALP assay kit was used to measure ALP activity in serum. (c) The mRNA levels of *Mgat5* in vertebrae and femur were quantified by qPCR. (d) Representative western blot images of MGAT5 expression in vertebrae and femur. (e) qPCR was used to detect the mRNA level of *Runx2*, *Ocn* and *Osx* in vertebrae and femur. (f) Protein expression of RUNX2, OCN and OSX was measured by western blotting analysis. All values were shown as mean ± SD (n=6). Statistical significance was defined at $P<0.05$. MGAT5, N-acetylglucosaminyltransferase V; OVX, ovariectomized; OP, osteoporosis; micro-CT, micro-computed tomography; BMD, bone mass density; BV/TV, ratio of bone volume to total volume; Tb.N, trabecular number; ALP, alkaline phosphatase; qPCR, quantitative real-time PCR; RUNX2, RUNX family transcription factor 2; OCN, osteocalcin; OSX, osterix.

Table 2. Bone parameters in the femur

	Control (n=6)	OP (n=6)
N.Oc	4.50 ± 0.55	14.00 ± 1.55[a]
Oc.S (μm^2)	4,032.33 ± 643.61	26,222.00 ± 3,012.78[a]
N.Ob	92.17 ± 9.91	29.00 ± 3.22[a]
Ob.S (μm^2)	54,371.17 ± 6,728.44	10,801.50 ± 1,481.38[a]

N.Oc, osteoclast number; Oc.S, osteoclast surface; N.Ob, osteoblast number; Ob.S, osteoblast surface. [a]$P<0.001$ compared with the control group.

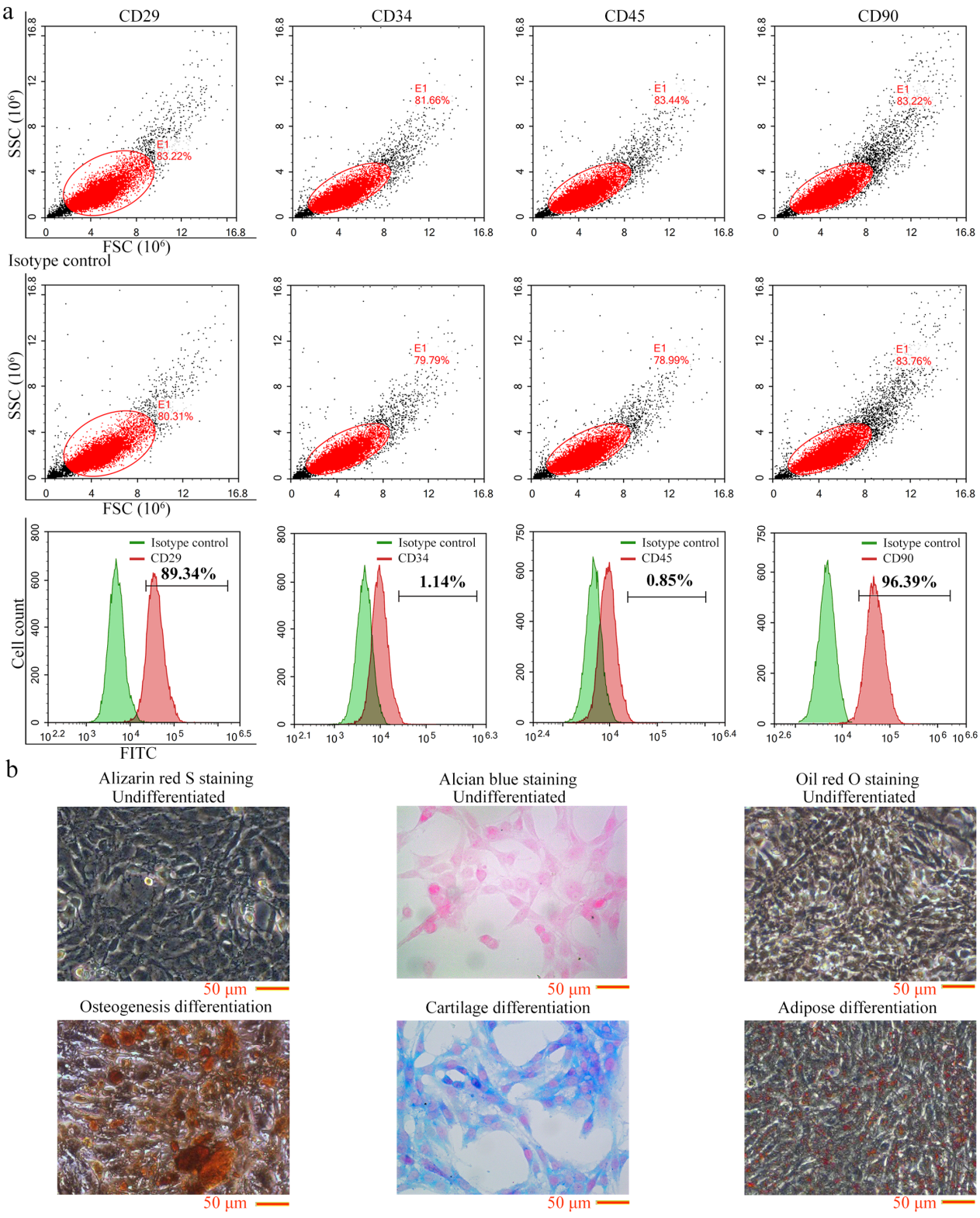

Fig. 2. Identification and differentiation of BMSCs. (a) Representative flow cytometry dot-plots and histograms showing high expression levels of CD29 and CD90 and low expression levels of CD34 and CD45 on the surface of BMSCs. (b) The differentiation capacity of BMSCs to differentiate into the osteogenic, adipogenic, and chondrogenic lineages was determined by Alizarin red S staining (left panel, scale bar: 50 μm), Alcian blue staining (middle panel, scale bar: 50 μm) and Oil Red O staining (right panel, scale bar: 50 μm), respectively. Top panels showed the Alizarin red S staining, Alcian blue staining and Oil Red O staining of undifferentiated BMSCs as negative controls. BMSCs, bone marrow mesenchymal stem cells.

 doi: 10.1538/expanim.22-0129

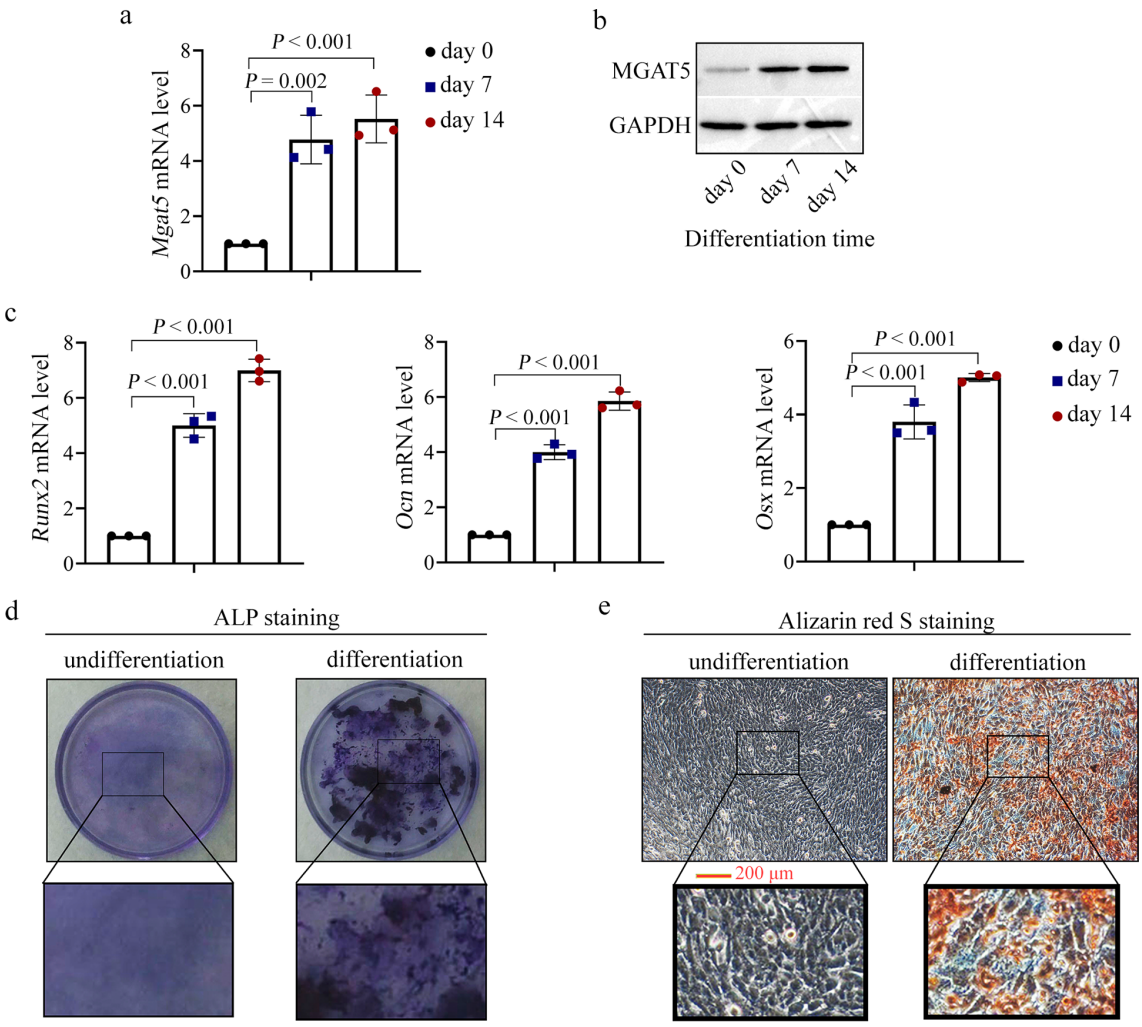

Fig. 3. Up-regulated expression of MGAT5 during the osteogenic differentiation and mineralization of BMSCs. (a, b) *Mgat5* mRNA expression levels and MGAT5 protein expression levels were determined by qPCR and western blotting analysis at day 0, 7, and 14 of osteogenic differentiation. (c) The mRNA levels of *Runx2*, *Ocn* and *Osx* were detected by qPCR at day 0, 7 and 14 after osteogenic induction of BMSCs. (d) Representative images of ALP staining after BMSCs treated with osteoblast differentiation medium for 7 days. (e) Representative images of Alizarin red S staining after BMSCs treated with osteoblast differentiation medium for 14 days (scale bar: 200 μm). Data were given as mean ± SD (n=3). Statistical significance was defined at $P<0.05$. MGAT5, N-acetylglucosaminyltransferase V; RUNX2, RUNX family transcription factor 2; OCN, osteocalcin; OSX, osterix; qPCR, quantitative real-time PCR; ALP, alkaline phosphatase; BMSCs, bone marrow mesenchymal stem cells.

Discussion

OP was aroused by low bone density and was complicated by fractures. The disfunction of osteoblasts were accepted as major pathogenic mechanisms of OP [21]. An abrupt cessation of estrogen after the menopause is one of the reasons to induce this reduction [22]. Therefore, we used the OVX mice, which were one of the most reliable models for researching primary OP, as a model to simulate postmenopausal woman with OP. MGAT5 is a glycosyl transferase that modulates cell growth and differentiation [23]. In our study, we found that the expression of MGAT5 was markedly reduced in the vertebra and femur tissues of OP mice and was accompanied by the loss of bone mass density and osteogenic markers. It is reported that the expression of MGAT5 was inhibited by nuclear factor kappa B (NF-κB), which is activated by ovariectomy [24, 25]. On the other hand, IL-10, whose expression is decreased in OVX mice [26], induced the expression of MGAT5 [27]. Thus, we speculated that the activated NF-κB or decreased IL-10 may contribute to the low MGAT5 expression in OVX condition. There may be other factors that influence the expression of MGAT5 in OP and need further exploration. Decreased ALP expression in bone represented reduced osteogenic differentiation [28], and increased ALP activity in serum might be caused by accelerated bone turnover and complex internal environment. Previous studies

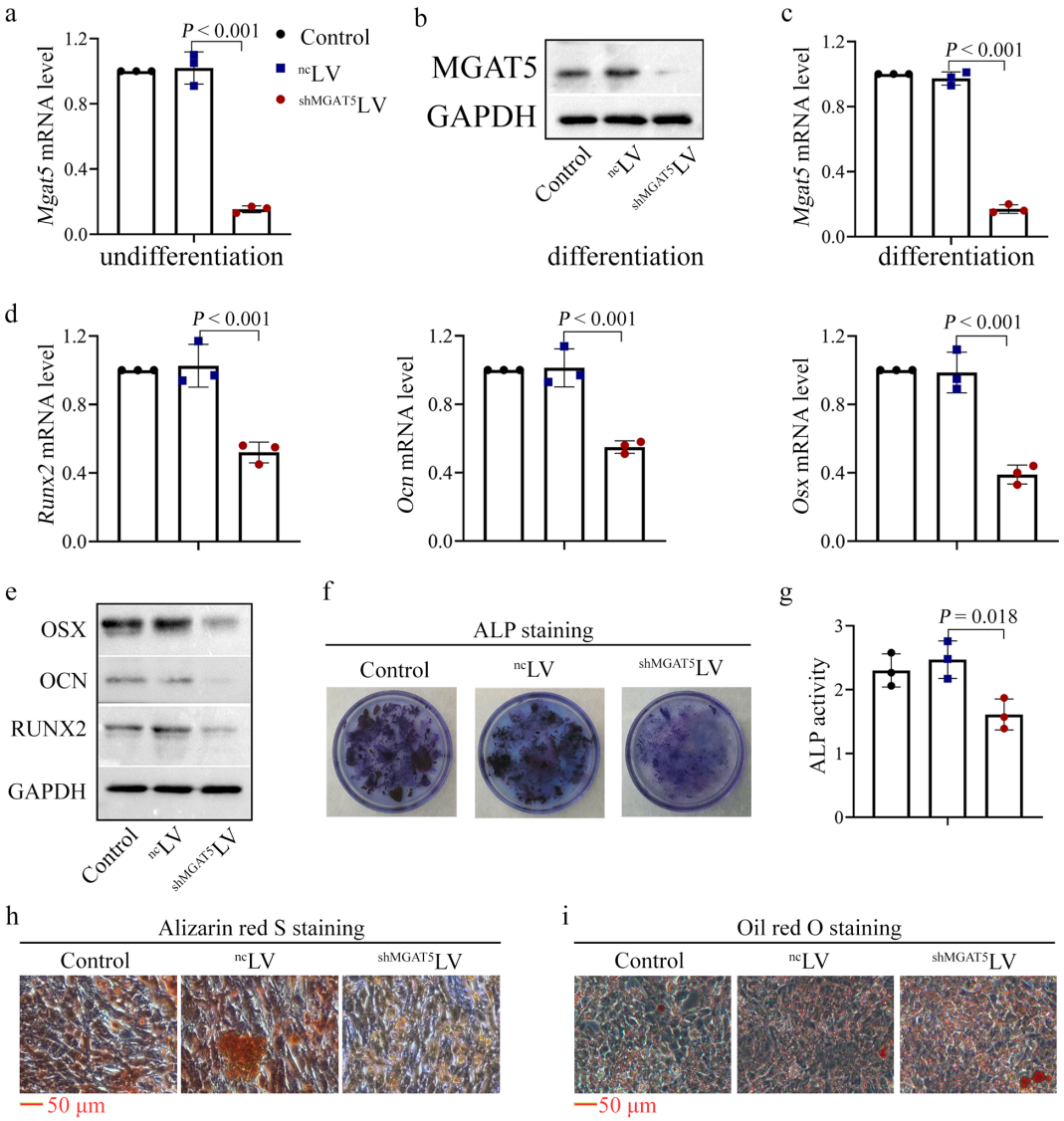

Fig. 4. *Mgat5* knockdown inhibited osteogenic differentiation of BMSCs. (a) The expression of *Mgat5* was determined by qPCR in the control group, the ^{nc}LV group and the ^{shMGAT5}LV group at 48 h of *Mgat5* knockdown. (b, c) *Mgat5* mRNA expression levels and MGAT5 protein expression levels were determined by qPCR and western blotting analysis in the control group, the ^{nc}LV group and the ^{shMGAT5}LV group at day 7 of osteogenic differentiation. (d) The mRNA levels of *Runx2*, *Ocn* and *Osx* were detected by qPCR in the control group, the ^{nc}LV group and the ^{shMGAT5}LV group at day 7 of osteogenic differentiation. (e) The protein expression levels of RUNX2, OCN and OSX were detected by western blotting analysis in the control group, the ^{nc}LV group and the ^{shMGAT5}LV group at day 7 of osteogenic differentiation. (f) Representative images of ALP staining in the control group, the ^{nc}LV group and the ^{shMGAT5}LV group after BMSCs treated with osteoblast differentiation medium for 7 days. (g) ALP activity in the control group, the ^{nc}LV group and the ^{shMGAT5}LV group at day 7 of osteogenic differentiation. (h) Representative images of Alizarin red S staining in the control group, the ^{nc}LV group and the ^{shMGAT5}LV group at day 14 of osteogenic differentiation (scale bar: 50 μm). (i) Representative images of Oil red O staining in the control group, the ^{nc}LV group and the ^{shMGAT5}LV group at day 14 of adipogenic differentiation (scale bar: 50 μm). Data were presented as mean ± SD (n=3). Statistical significance was defined at $P<0.05$. MGAT5, N-acetylglucosaminyltransferase V; RUNX2, RUNX family transcription factor 2; OCN, osteocalcin; OSX, osterix; qPCR, quantitative real-time PCR; ALP, alkaline phosphatase; BMSCs, bone marrow mesenchymal stem cells.

have shown that the mRNA and protein levels of ALP in the tibiae and femur of the OVX model were reduced [28, 29], which was consistent with our findings. Interestingly, most studies have measured ALP activity in serum and they revealed that ALP activity in serum was increased in OVX model [30–35]. Mukaiyama *et al.* proposed that in postmenopausal women, elevated ALP is caused by high bone turnover [36]. The vast majority of ALP activity of serum is derived from bone and liver [37]. These studies suggested that the ALP activity in serum was regulated by various factors *in vivo*. The exact cause of opposite presentation results of ALP activity (in serum) and expression (in bone) will be explored in our future study. In addition, Cheung *et al.* found that

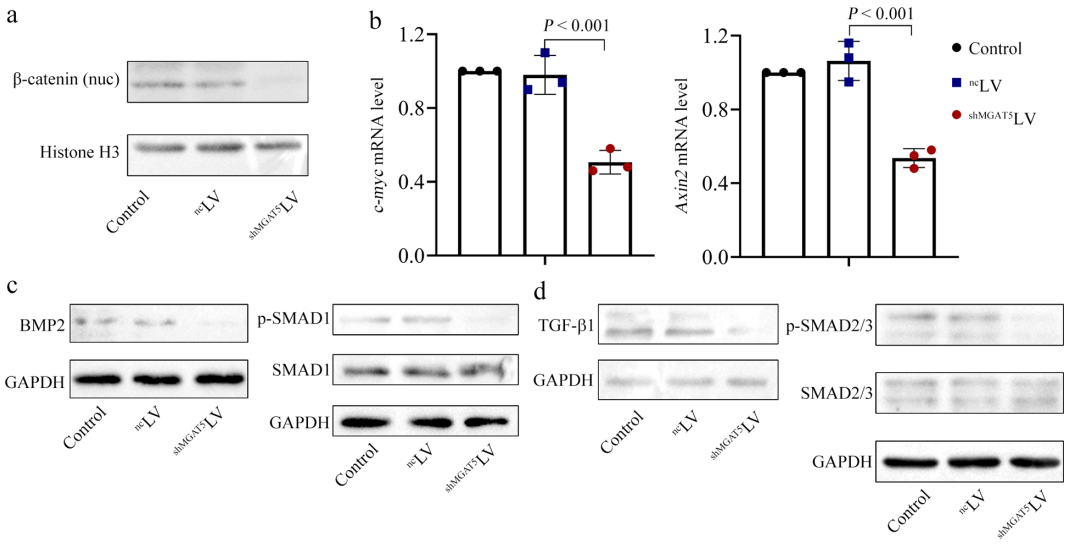

Fig. 5. *Mgat5* knockdown inhibited the Wnt/*β*-catenin and BMP/TGF-β signaling pathways. (a) Representative western blot showed the relative expression level of *β*-catenin in the control group, the ^{nc}LV group and the ^{shMGAT5}LV group. (b) The mRNA levels of *c-myc* and *Axin2* were detected by qPCR in the control group, the ^{nc}LV group and the ^{shMGAT5}LV group at day 7 of osteogenic differentiation. (c) Protein expression of BMP2 and phosphorylation of SMAD1 in the control group, the ^{nc}LV group and the ^{shMGAT5}LV group were assessed by western blot. (d) Western blot was used to detect the protein expression of TGF-β1 and phosphorylation of SMAD2/3 in the control group, the ^{nc}LV group and the ^{shMGAT5}LV group. Data were shown as mean ± SD (n=3). Statistical significance was defined at $P<0.05$. MGAT5, N-acetylglucosaminyltransferase V; *Axin2*, axis inhibition protein 2; qPCR, quantitative real-time PCR; BMP2, bone morphogenetic protein type 2; TGF-β1, transforming growth factor-β1.

deficiency of *Mgat5* resulted in damaged osteogenic differentiation of bone marrow, and accelerated loss of bone mass with aging [19]. Chen *et al.* denoted that MGAT5 promoted early osteogenic differentiation of stem cells and increase mRNA expression of osteogenic differentiation marker genes [23]. Together with our findings, MGAT5 might be involved in the development of OP and related to osteogenic differentiation of BMSCs.

Stem cells play an important role in the development of OP. Wang *et al.* found that in the osteoporosis model, stem cells with osteogenic differentiation potential could stably differentiate and improve the reduction in bone density [38]. MSC transplantation in OP treatment raised osteogenic differentiation and halt the deterioration of OP [39]. Previous study demonstrated that after promoting osteogenic differentiation of BMSCs, OP development in mouse model was repressed [40]. In our study, MGAT5 was found to be upregulated when the BMSCs underwent osteogenic differentiation, along with these osteogenic protein markers. The upregulation sustained to day 14, the time point mineralization occurred. MGAT5-mediated N-glycosylation, a common post-translational modification of proteins, affects cell growth, differentiation and migration [41]. N-glycans produced by MGAT5 adapted cellular sensitivities to cytokine, thereby modulating osteogenic activity [19]. Mice with insufficient N-glycan synthesis shown osteogenic abnormalities [42]. In addition, osteogenic differentiation of dental pulp stem cells was dependent on MGAT5 through regulating N-glycan-branching TGF-β receptor type I level [23]. Our and previous observations strongly indicated that MGAT5 served functions in osteogenic differentiation of BMSCs. Therefore, we established *Mgat5*-silencing BMSCs to test our hypothesis. As expected, the BMSCs lack of *Mgat5* showed an obviously inhibited osteogenic differentiation ability compared with the normal BMSCs. Meanwhile, the expression of osteogenic markers was decreased and the mineralization was suppressed. These findings suggested that loss of *Mgat5* was detrimental to osteogenic differentiation. The osteogenic differentiation of BMSCs was regulated by multiple transcription factors. RUNX2 and OSX were critical for regulating the osteogenesis-specific proteins (including ALP and OCN) and ultimately stimulated mineralization of bone nodules, that were essential for osteoblast proliferation and bone formation [43]. OCN appeared at the end stage of osteoblast differentiation. It could bind to Ca^{2+} to regulate calcium ion homeostasis and bone mineralization [44]. ALP activity was the most widely recognized marker of osteoblast activity. It was a typical protein product of osteoblast phenotype and osteoblast differentiation [45]. Generally, the appearance of ALP activity represented a phenotypic marker of osteoblast formation because it provided necessary phosphoric acid for the formation of apatite via hydrolyzing phosphate [46, 47]. In our observations, osteogenic

medium-induced increases of these proteins in BMSCs were suppressed when *Mgat5* was silenced, indicating that MGAT5 may modulate the transcription of these factors. Given that MGAT5 is not a transcriptional factor, it may exert this regulation indirectly through other transcriptional factors, which is worthy to be further investigated. In human post-menopausal OP, increased adipogenesis in bone marrow is observed [48]. Previous studies proposed that the adipogenic differentiation of BMSCs obtained from OVX mice was increased and the increase contributed to OP [49, 50]. Our results proved that the adipogenic differentiation of BMSCs was enhanced by *Mgat5* knockdown, thereby aggravating OP.

Canonical Wnt signaling plays an essential role in osteoblastgenesis and skeletal development [51]. It determines the fate of MSCs by preventing their adipogenic and chondrogenic differentiation and promoting the osteogenic differentiation [52]. As a key component of the Wnt signaling pathway, *β*-catenin is involved in these biological processes and its inactivation is related with bone metabolism disorders. Accumulating evidence suggested that activation of *β*-catenin promoted osteogenic differentiation of BMSCs [53–55]. The expression of MGAT5 was found to be positively related to nuclear translocation of *β*-catenin [56], suggesting the possible regulatory relationship between these two proteins. In line with this finding, our study also observed the inhibited level of *β*-catenin in the nucleus in *Mgat5* silencing cells, as well as the decreased expressions of downstream genes *c-myc* and *Axin2*, both of which were associated with bone development and osteogenic differentiation of BMSCs [57, 58]. On the other hand, BMP and TGF-β are the main signaling pathways in bone formation and osteogenesis [59]. The BMP performs its function through downstream transcription factors including SMAD1. Phosphorylation of SMAD2 and SMAD3 initiates the TGF-β signal transduction [60]. Once SMADs are phosphorylated, they form complex with SMAD4. This complex activates the transcription and then stimulates bone formation [61]. Our results demonstrated that *Mgat5* knockdown inhibited the BMP/TGF-β signaling pathways. Previous study attested our findings. Chen *et al.* revealed that MGAT5 played a key role in activating TGF-β signaling pathway and subsequent osteogenic differentiation [23]. Therefore, our findings indicated that MGAT5 might be involved in osteogenic differentiation of BMSCs through modulating Wnt/*β*-catenin and BMP/TGF-β signaling pathways. While how does it regulate the expressions of those osteogenic genes, and whether it directly modulates *β*-catenin activity, or indirectly through other factors, still need to be revealed.

Conclusion

In conclusion, MGAT5 may regulate the osteogenic differentiation of BMSCs through *β*-catenin and BMP/TGF-β signaling pathways. Loss of it may be associated with the development of OP.

Competing Interests

The authors have no competing interests to declare that are relevant to the content of this article.

References

1. Starling S. New anti-osteoporosis drug target identified. Nat Rev Endocrinol. 2021; 17: 4–5. [Medline] [CrossRef]
2. Lyu H, Yoshida K, Zhao SS, Wei J, Zeng C, Tedeschi SK, et al. Delayed denosumab injections and fracture risk among patients with osteoporosis: a population-based cohort study. Ann Intern Med. 2020; 173: 516–526. [Medline] [CrossRef]
3. Rachner TD, Khosla S, Hofbauer LC. Osteoporosis: now and the future. Lancet. 2011; 377: 1276–1287. [Medline] [CrossRef]
4. Crandall CJ, Larson J, Wright NC, Laddu D, Stefanick ML, Kaunitz AM, et al. Serial bone density measurement and incident fracture risk discrimination in postmenopausal women. JAMA Intern Med. 2020; 180: 1232–1240. [Medline] [CrossRef]
5. Shih YV, Liu M, Kwon SK, Iida M, Gong Y, Sangaj N, et al. Dysregulation of ectonucleotidase-mediated extracellular adenosine during postmenopausal bone loss. Sci Adv. 2019; 5: eaax1387. [Medline] [CrossRef]
6. Tella SH, Gallagher JC. Prevention and treatment of postmenopausal osteoporosis. J Steroid Biochem Mol Biol. 2014; 142: 155–170. [Medline] [CrossRef]
7. Liu Y, Yu P, Peng X, Huang Q, Ding M, Chen Y, et al. Hexapeptide-conjugated calcitonin for targeted therapy of osteoporosis. J Control Release. 2019; 304: 39–50. [Medline] [CrossRef]
8. Lee S, Kim GJ, Kwon H, Nam JW, Baek JY, Shim SH, et al. Estrogenic effects of extracts and isolated compounds from belowground and aerial parts of spartina anglica. Mar Drugs. 2021; 19: 210. [Medline] [CrossRef]
9. Hagino H, Sugimoto T, Tanaka S, Sasaki K, Sone T, Nakamura T, et al. A randomized, controlled trial of once-weekly teriparatide injection versus alendronate in patients at high risk of osteoporotic fracture: primary results of the Japanese Osteoporosis Intervention Trial-05. Osteoporos Int. 2021; 32: 2301–2311. [Medline] [CrossRef]
10. Choi D, Choi S, Chang J, Park SM. Exposure to oral bisphosphonates and risk of gastrointestinal cancer. Osteoporos Int. 2020; 31: 775–782. [Medline] [CrossRef]
11. Zeytinoglu M, Naaman SC, Dickens LT. Denosumab discontinuation in patients treated for low bone density and osteoporosis. Endocrinol Metab Clin North Am. 2021; 50: 205–222. [Medline] [CrossRef]
12. Eastell R, O'Neill TW, Hofbauer LC, Langdahl B, Reid IR, Gold DT, et al. Postmenopausal osteoporosis. Nat Rev Dis Primers. 2016; 2: 16069. [Medline] [CrossRef]
13. Raterman HG, Bultink IE, Lems WF. Osteoporosis in patients with rheumatoid arthritis: an update in epidemiology, pathogenesis, and fracture prevention. Expert Opin Pharmacother. 2020; 21: 1725–1737. [Medline] [CrossRef]
14. Grayson WL, Bunnell BA, Martin E, Frazier T, Hung BP, Gimble JM. Stromal cells and stem cells in clinical bone regeneration. Nat Rev Endocrinol. 2015; 11: 140–150. [Medline] [CrossRef]

15. Qi Q, Wang Y, Wang X, Yang J, Xie Y, Zhou J, et al. Histone demethylase KDM4A regulates adipogenic and osteogenic differentiation via epigenetic regulation of C/EBPα and canonical Wnt signaling. Cell Mol Life Sci. 2020; 77: 2407–2421. [Medline] [CrossRef]
16. Chen X, Zhi X, Wang J, Su J. RANKL signaling in bone marrow mesenchymal stem cells negatively regulates osteoblastic bone formation. Bone Res. 2018; 6: 34. [Medline] [CrossRef]
17. Zheng CX, Sui BD, Qiu XY, Hu CH, Jin Y. Mitochondrial regulation of stem cells in bone homeostasis. Trends Mol Med. 2020; 26: 89–104. [Medline] [CrossRef]
18. Yan G, Li Y, Zhan L, Sun S, Yuan J, Wang T, et al. Decreased miR-124-3p promoted breast cancer proliferation and metastasis by targeting MGAT5. Am J Cancer Res. 2019; 9: 585–596. [Medline]
19. Cheung P, Pawling J, Partridge EA, Sukhu B, Grynpas M, Dennis JW. Metabolic homeostasis and tissue renewal are dependent on beta1,6GlcNAc-branched N-glycans. Glycobiology. 2007; 17: 828–837. [Medline] [CrossRef]
20. Abdallah BM, Jafari A, Zaher W, Qiu W, Kassem M. Skeletal (stromal) stem cells: an update on intracellular signaling pathways controlling osteoblast differentiation. Bone. 2015; 70: 28–36. [Medline] [CrossRef]
21. Rosen CJ, Klibanski A. Bone, fat, and body composition: evolving concepts in the pathogenesis of osteoporosis. Am J Med. 2009; 122: 409–414. [Medline] [CrossRef]
22. Liu X, Liu H, Xiong Y, Yang L, Wang C, Zhang R, et al. Postmenopausal osteoporosis is associated with the regulation of SP, CGRP, VIP, and NPY. Biomed Pharmacother. 2018; 104: 742–750. [Medline] [CrossRef]
23. Chen YJ, Yao CC, Huang CH, Chang HH, Young TH. Hexosamine-induced TGF-beta signaling and osteogenic differentiation of dental pulp stem cells are dependent on N-acetylglucosaminyltransferase V. BioMed Res Int. 2015; 2015: 924397. [Medline] [CrossRef]
24. Mahmoud AM, Ali MM. High glucose and advanced glycation end products induce CD147-mediated mmp activity in human adipocytes. Cells. 2021; 10: 2098. [Medline] [CrossRef]
25. Xu Y, Sheng H, Bao Q, Wang Y, Lu J, Ni X. NLRP3 inflammasome activation mediates estrogen deficiency-induced depression- and anxiety-like behavior and hippocampal inflammation in mice. Brain Behav Immun. 2016; 56: 175–186. [Medline] [CrossRef]
26. Chen X, Zhang Z, Hu Y, Cui J, Zhi X, Li X, et al. Lactulose suppresses osteoclastogenesis and ameliorates estrogen deficiency-induced bone loss in mice. Aging Dis. 2020; 11: 629–641. [Medline] [CrossRef]
27. Smith LK, Boukhaled GM, Condotta SA, Mazouz S, Guthmiller JJ, Vijay R, et al. Interleukin-10 directly inhibits CD8(+) T cell function by enhancing N-glycan branching to decrease antigen sensitivity. Immunity. 2018; 48: 299–312.e5. [Medline] [CrossRef]
28. Yang N, Zhang X, Li L, Xu T, Li M, Zhao Q, et al. Ginsenoside rc promotes bone formation in ovariectomy-induced osteoporosis in vivo and osteogenic differentiation in vitro. Int J Mol Sci. 2022; 23: 6187. [Medline]
29. Zhao R, Zhou Y, Li J, Lin J, Cui W, Peng Y, et al. Irisin regulating skeletal response to endurance exercise in ovariectomized mice by promoting Akt/beta-catenin pathway. Front Physiol. 2021; 12: 639066. [Medline] [CrossRef]
30. Zhang R, Hu SJ, Li C, Zhang F, Gan HQ, Mei QB. Achyranthes bidentata root extract prevent OVX-induced osteoporosis in rats. J Ethnopharmacol. 2012; 139: 12–18. [Medline] [CrossRef]
31. Sun X, Wei B, Peng Z, Chen X, Fu Q, Wang C, et al. A polysaccharide from the dried rhizome of Drynaria fortunei (Kunze) J. Sm. prevents ovariectomized (OVX)-induced osteoporosis in rats. J Cell Mol Med. 2020; 24: 3692–3700. [Medline] [CrossRef]
32. Lim DW, Kim JG, Lee Y, Cha SH, Kim YT. Preventive effects of Eleutherococcus senticosus bark extract in OVX-induced osteoporosis in rats. Molecules. 2013; 18: 7998–8008. [Medline] [CrossRef]
33. Shaban NZ, Talaat IM, Elrashidy FH, Hegazy AY, Sultan AS. Therapeutic role of punica granatum (pomegranate) seed oil extract on bone turnover and resorption induced in ovariectomized rats. J Nutr Health Aging. 2017; 21: 1299–1306. [Medline] [CrossRef]
34. Wang X, Wang M, Cui X, Li Z, Guo S, Gao F, et al. Antiosteoporosis effect of geraniin on ovariectomy-induced osteoporosis in experimental rats. J Biochem Mol Toxicol. 2021; 35: 1–8. [Medline]
35. Cheng M, Wang Q, Fan Y, Liu X, Wang L, Xie R, et al. A traditional Chinese herbal preparation, Er-Zhi-Wan, prevent ovariectomy-induced osteoporosis in rats. J Ethnopharmacol. 2011; 138: 279–285. [Medline] [CrossRef]
36. Mukaiyama K, Kamimura M, Uchiyama S, Ikegami S, Nakamura Y, Kato H. Elevation of serum alkaline phosphatase (ALP) level in postmenopausal women is caused by high bone turnover. Aging Clin Exp Res. 2015; 27: 413–418. [Medline] [CrossRef]
37. Levitt MD, Hapak SM, Levitt DG. Alkaline Phosphatase Pathophysiology with Emphasis on the Seldom-Discussed Role of Defective Elimination in Unexplained Elevations of Serum ALP - A Case Report and Literature Review. Clin Exp Gastroenterol. 2022; 15: 41–49. [Medline] [CrossRef]
38. Wang Z, Wang D, Liu Y, Liu D, Ren Y, Liu Z, et al. Mesenchymal stem cell in mice uterine and its therapeutic effect on osteoporosis. Rejuvenation Res. 2021; 24: 139–150. [Medline] [CrossRef]
39. Jiang Y, Zhang P, Zhang X, Lv L, Zhou Y. Advances in mesenchymal stem cell transplantation for the treatment of osteoporosis. Cell Prolif. 2021; 54: e12956. [Medline] [CrossRef]
40. Wang X, Chen T, Deng Z, Gao W, Liang T, Qiu X, et al. Melatonin promotes bone marrow mesenchymal stem cell osteogenic differentiation and prevents osteoporosis development through modulating circ_0003865 that sponges miR-3653-3p. Stem Cell Res Ther. 2021; 12: 150. [Medline] [CrossRef]
41. Mikolajczyk K, Kaczmarek R, Czerwinski M. How glycosylation affects glycosylation: the role of N-glycans in glycosyltransferase activity. Glycobiology. 2020; 30: 941–969. [Medline] [CrossRef]
42. Wang Y, Schachter H, Marth JD. Mice with a homozygous deletion of the Mgat2 gene encoding UDP-N-acetylglucosamine:alpha-6-D-mannoside beta1,2-N-acetylglucosaminyltransferase II: a model for congenital disorder of glycosylation type IIa. Biochim Biophys Acta. 2002; 1573: 301–311. [Medline] [CrossRef]
43. An J, Yang H, Zhang Q, Liu C, Zhao J, Zhang L, et al. Natural products for treatment of osteoporosis: The effects and mechanisms on promoting osteoblast-mediated bone formation. Life Sci. 2016; 147: 46–58. [Medline] [CrossRef]
44. Ducy P, Desbois C, Boyce B, Pinero G, Story B, Dunstan C, et al. Increased bone formation in osteocalcin-deficient mice. Nature. 1996; 382: 448–452. [Medline] [CrossRef]
45. Bremner I, Beattie JH. Copper and zinc metabolism in health and disease: speciation and interactions. Proc Nutr Soc. 1995; 54: 489–499. [Medline] [CrossRef]
46. Stein GS, Lian JB, Owen TA. Relationship of cell growth to the regulation of tissue-specific gene expression during osteoblast differentiation. FASEB J. 1990; 4: 3111–3123. [Medline] [CrossRef]
47. Niu LN, Sun JQ, Li QH, Jiao K, Shen LJ, Wu D, et al. Intrafibrillar-silicified collagen scaffolds enhance the osteogenic capacity of human dental pulp stem cells. J Dent. 2014; 42: 839–849. [Medline] [CrossRef]
48. Fu Y, Li R, Zhong J, Fu N, Wei X, Cun X, et al. Adipogenic differentiation potential of adipose-derived mesenchymal stem cells from ovariectomized mice. Cell Prolif. 2014; 47:

604–614. [Medline] [CrossRef]
49. Qi M, Zhang L, Ma Y, Shuai Y, Li L, Luo K, et al. Autophagy maintains the function of bone marrow mesenchymal stem cells to prevent estrogen deficiency-induced osteoporosis. Theranostics. 2017; 7: 4498–4516. [Medline] [CrossRef]
50. Yu X, Song MS, Rong PZ, Chen XJ, Shi L, Wang CH, et al. LncRNA SNHG1 modulates adipogenic differentiation of BMSCs by promoting DNMT1 mediated Opg hypermethylation via interacting with PTBP1. J Cell Mol Med. 2022; 26: 60–74. [Medline] [CrossRef]
51. Teufel S, Hartmann C. Wnt-signaling in skeletal development. Curr Top Dev Biol. 2019; 133: 235–279. [Medline] [CrossRef]
52. Rossini M, Gatti D, Adami S. Involvement of WNT/β-catenin signaling in the treatment of osteoporosis. Calcif Tissue Int. 2013; 93: 121–132. [Medline] [CrossRef]
53. Shares BH, Busch M, White N, Shum L, Eliseev RA. Active mitochondria support osteogenic differentiation by stimulating β-catenin acetylation. J Biol Chem. 2018; 293: 16019–16027. [Medline] [CrossRef]
54. Wang Y, Zhang X, Shao J, Liu H, Liu X, Luo E. Adiponectin regulates BMSC osteogenic differentiation and osteogenesis through the Wnt/β-catenin pathway. Sci Rep. 2017; 7: 3652. [Medline] [CrossRef]
55. Zhao SJ, Kong FQ, Jie J, Li Q, Liu H, Xu AD, et al. Macrophage MSR1 promotes BMSC osteogenic differentiation and M2-like polarization by activating PI3K/AKT/GSK3β/β-catenin pathway. Theranostics. 2020; 10: 17–35. [Medline] [CrossRef]
56. Guo H, Nagy T, Pierce M. Post-translational glycoprotein modifications regulate colon cancer stem cells and colon adenoma progression in Apc(min/+) mice through altered Wnt receptor signaling. J Biol Chem. 2014; 289: 31534–31549. [Medline] [CrossRef]
57. Shen JJ, Zhang CH, Chen ZW, Wang ZX, Yang DC, Zhang FL, et al. LncRNA HOTAIR inhibited osteogenic differentiation of BMSCs by regulating Wnt/β-catenin pathway. Eur Rev Med Pharmacol Sci. 2019; 23: 7232–7246. [Medline]
58. Hsu YH, Kiel DP. Clinical review: Genome-wide association studies of skeletal phenotypes: what we have learned and where we are headed. J Clin Endocrinol Metab. 2012; 97: E1958–E1977. [Medline] [CrossRef]
59. Zhao B, Xing G, Wang A. The BMP signaling pathway enhances the osteoblastic differentiation of bone marrow mesenchymal stem cells in rats with osteoporosis. J Orthop Surg Res. 2019; 14: 462. [Medline] [CrossRef]
60. Sakou T, Onishi T, Yamamoto T, Nagamine T, Sampath T, Ten Dijke P. Localization of Smads, the TGF-beta family intracellular signaling components during endochondral ossification. J Bone Miner Res. 1999; 14: 1145–1152. [Medline] [CrossRef]
61. Nohe A, Keating E, Knaus P, Petersen NO. Signal transduction of bone morphogenetic protein receptors. Cell Signal. 2004; 16: 291–299. [Medline] [CrossRef]